Springer

Journal of
Mechanical
Science and
Technology

Journal of Mechanical Science and Technology 23 (2009) 1670~1679

www.springerlink.com/content/1738-494x
DOI 10.1007/s12206-009-0417-1

Measurements of the characteristics of spray droplets using in-line digital particle holography †

Yan Yang[1,2] and Boseon Kang[2,*]

[1]*Key Lab. of Automobile Parts & Test Technique of Ministry of Education, Chongqing University of Technology, 400050, china*
[2]*Dept. of Mechanical Systems Engineering, Chonnam National Univ., 500-757, Korea*

(Manuscript Received June 30, 2008; Revised February 23, 2009; Accepted March 2, 2009)

Abstract

In-line digital particle holography is applied to measure the characteristics of spray droplets. Common reconstruction methods were considered and the best one was selected. Several important parameters at the time of hologram recording, such as the object distance and the region of laser beam used, are discussed. The feasibility of the correlation coefficient (CC) method for focal plane determination of 3-D droplets was verified. A double exposure hologram recording system with synchronization system for time control was established, and two digital spray holograms were obtained in a short time interval. For post-processing of reconstruction images, the two-threshold and the image segmentation methods were used in binary image transformation. Using the CC method and some image processing techniques applied to droplets in each double exposure image, the spatial positions of droplets used to evaluate the three dimensional droplet velocities were easily located, which proved the feasibility of in-line digital particle holographic technology as a good measurement tool for spray droplets.

Keywords: Digital particle; Holography; Spray droplets; Correlation coefficient method

1. Introduction

Holography allows the light scattered from an object to be recorded and later reconstructed, thereby appearing as if the object is in the same position relative to the recording medium as when it was recorded. It can instantaneously capture volumetric information of 3-D fields. Due to the rapid development of digital technology, digital holography is taking the place of conventional optical holography. Digital holography does not need the physical or chemical processes of conventional holography, and its benefits are high efficiency, simplicity, and the ability to perform real time analysis. Therefore, it can be used in many practical measurement fields [1].

There are many techniques for analyzing the features of particle sizes, spatial distributions, and velocities. A commonly used laser instrument is the phase doppler anemometer, but it is a point measurement method. Particle image velocimetry, which can detect particles in a two-dimensional plane, can overcome this problem. Digital particle holography is a good solution which can obtain a three-dimensional recording of particles. Due to the rapid development of CCD cameras and computer technologies, the quality of holograms is becoming better and the computing speed of image reconstruction is becoming faster. Therefore, digital particle holography has strong potential in the measurement of particle features.

The key points in digital particle holographic technology are high resolution, an appropriate reconstruction method, post-processing of reconstruction images, and focal plane determination. Jaquot et al. [2] showed some techniques for high resolution hologra-

† This paper was recommended for publication in revised form by Associate Editor Gihun Son
*Corresponding author. Tel.: +82 62 530 1683, Fax.: +82 62 530 1689
E-mail address: bskang@chonnam.ac.kr

phy, Lai et al. [3] developed a method to obtain high quality reconstruction images, and Wang et al. [4] investigated the optimal recording condition of holograms. Schnars and Jueptner [1] presented several common reconstruction methods. The post-processing of reconstruction images is an image processing procedure, and many methods have been discussed [5, 6]. In addition, various methods have been developed for focal plane location. Yu and Cai investigated a criterion based on gradient computation [7]. Dubois et al. introduced a method that uses the score of the integrated amplitude modulus [8]. Lefebvre et al. showed that the maximum modulus of the wavelet transform was reached at the best focal plane [9]. Zhang et al. located the focal plane using the Gabor transform [10], and Yang et al. presented the correlation coefficient (CC) method and verified it using 2-D calibration targets [11].

In this study, measurements of the characteristics of spray droplets are attempted by digital particle holography. Several important parameters for high quality hologram recording are investigated. The CC method for 3-D droplets was verified, and this method was applied to determine the focal plane of real spray droplets. A hologram recording system was designed to obtain double exposure holograms. In the post-processing of reconstruction images, the two-threshold and the image segmentation methods were used. After obtaining the x and y coordinates of each droplet in double exposure images using image processing techniques, we reconstructed every droplet and obtained the z coordinates by the CC method. Then, the three dimensional velocities of droplets were easily calculated.

2. General principles

2.1 Principle of digital holography

The procedure of digital holography, namely, hologram recording and object reconstruction, is similar to that of optical holography. However, digital holography has several obvious advantages over optical holography. The recording medium is a CCD camera instead of photographic film. The reconstruction of recorded holograms is achieved by computer, which is called numerical reconstruction.

Digital holography is classified as in-line or off-axis depending on the optical set-up. In-line digital holography is widely used because it has a simple optical configuration. The principle of in-line digital holography is shown in Fig. 1. An expanded laser beam goes through the object field. The part of beam diffracted by objects and arriving at the recording surface is the object beam, and the beam arriving without distortion by objects is the reference beam. The superposition of two beams creates an interference pattern on the CCD sensor. This diffraction can be described by the Fresnel-Kirchhoff integral [1],

$$R(\xi',\eta') = \frac{i}{\lambda}\int_{-\infty}^{\infty}\int_{-\infty}^{\infty} h(x,y)E_R(x,y)\frac{\exp(-i\frac{2\pi}{\lambda}\rho)}{\rho}dxdy \tag{1}$$

with

$$\rho = \sqrt{(\xi'-x)^2+(\eta'-y)^2+d^2} \tag{2}$$

where $R(\xi',\eta')$, $h(x,y)$, and $E_R(x,y)$ are functions of the reconstruction image, hologram, and reference beam, respectively; d is the distance between two adjacent planes, λ is the wavelength, and ρ is the distance between two corresponding points in these two adjacent planes. The coordinates appearing in Eqs. (1) and (2) are shown in Fig. 2.

2.2 Reconstruction methods

The Fresnel and convolution methods are usually used for reconstructing holograms [1]. Each method is a different expression of Eq. (1). The Fresnel method is expressed as

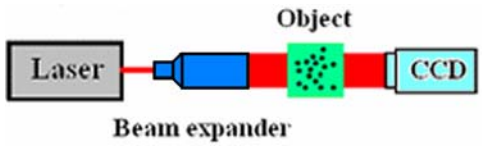

Fig. 1. Principle of in-line digital holography.

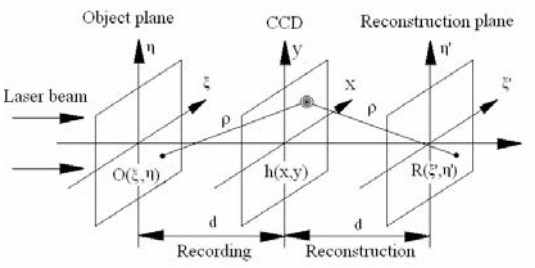

Fig. 2. Coordinate system.

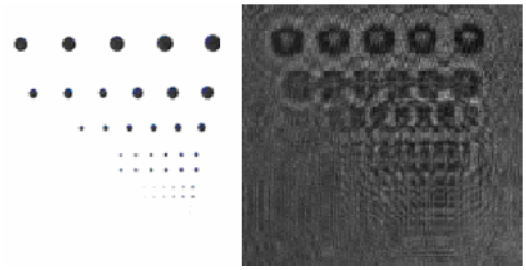

(a) real image (b) hologram

Fig. 3. A calibration target and its hologram (partial).

$$R(\xi',\eta') = \frac{i}{\lambda d}\exp(-i\frac{2\pi}{\lambda}d)\exp[-i\frac{\pi}{\lambda d}(\xi'^2+\eta'^2)] \cdot F^{-1}\{h(x,y)\exp[-i\frac{\pi}{\lambda d}(x^2+y^2)]\} \quad (3)$$

where $F^{-1}[]$ is an inverse Fourier transform. The expression for the convolution method is

$$R(\xi',\eta') = F^{-1}\{F[h(x,y)] \cdot F[\frac{i}{\lambda}\frac{\exp[-i\frac{2\pi}{\lambda}\sqrt{(d^2+(x-\xi')^2+(y-\eta')^2}]}{\sqrt{(d^2+(x-\xi')^2+(y-\eta')^2}}]\} \quad (4)$$

where $F[]$ is a Fourier transform.

A 2-D calibration target is used to determine which method is better because it is simpler than a real spray, and good as a test object. The real image and hologram of this target are shown in Fig. 3. After obtaining holograms at different distances, we reconstructed them by both methods, and the results are shown in Fig. 4.

In Fig. 4, the size of reconstruction image using the Fresnel method depended on the object distance (reconstruction distance), i.e., it changed with the object distance. On the other hand, the size does not change when we apply the convolution method to reconstruct the hologram. In the magnified reconstruction images, it is clearly shown that the quality of the reconstruction images by the convolution method is better than that of the Fresnel method. Therefore, the convolution method is selected as the reconstruction method.

2.3 Focal plane determination

Determining the focal plane of particles, i.e., the accurate positioning of particles along the optical axis, is the most important problem in digital particle holography because the reconstructed particle images have a long depth of focus. In this study, we applied the correlation coefficient (CC) method to locate droplet positions along the optical axis.

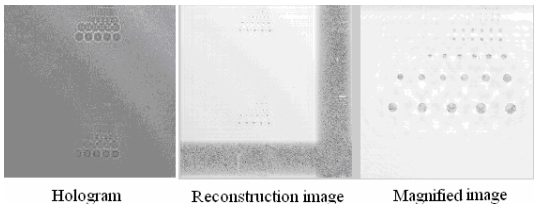

(a) Fresnel method (d=223.5 mm)

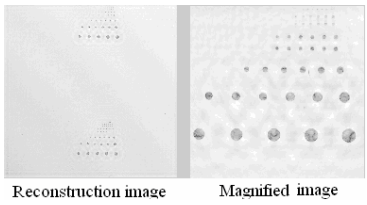

(b) convolution method (d=223.5 mm)

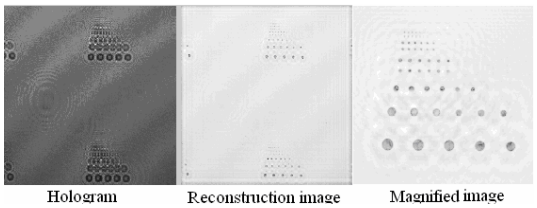

(c) Fresnel method (d =182 mm)

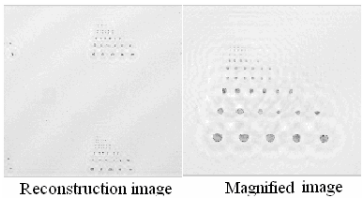

(d) convolution method (d =182 mm)

Fig. 4. Comparison of two reconstruction methods.

In optical holography, the CC method was first presented by Choo and Kang [12]. The correlation coefficient of images is a number between 0 and 1, which measures the degree to which two images are similar. The correlation coefficient is defined as

$$CC = \left| \frac{\sum_m \sum_n (F_{mn}-\overline{F})(G_{mn}-\overline{G})}{\sqrt{[\sum_m \sum_n (F_{mn}-\overline{F})^2][\sum_m \sum_n (G_{mn}-\overline{G})^2]}} \right| \quad (5)$$

where F and G are the images, m and n are the pixel indices, F_{mn} and G_{mn} are the gray levels of individual pixel of image F and G, and $\overline{F}$ and $\overline{G}$ are the mean gray levels of F and G. An image can be denoted by a matrix in the program so the values of F_{mn}, G_{mn}, $\overline{F}$, and $\overline{G}$ can be obtained easily after we import the image into the program. Fig. 5 shows schematically how to determine the focal plane of particles by using correlation coefficients. A series of images are reconstructed slice by slice with the reconstruction interval, Δz. The correlation coefficient of a particle on an arbitrary plane along the optical axis is evaluated by using two images at the same distance as half of the correlation interval, $\Delta C_z / 2$, from that plane. Two symmetrical images at each side of the focal plane should be most similar, and thus, the value of the correlation coefficient at the focal plane should be maximum. Therefore, the focal plane can be determined by choosing the peak point from the correlation coefficient curve.

The CC method has been verified in digital holography with the use of simulation holograms and 2-D dot objects [11]. In a real spray droplet field, droplets cannot be considered as simple plane dots. Therefore, we first verified the feasibility of the CC method for real 3-D droplet location, and then applied this method to the spray field. Fig. 6 shows the validation experiments to check the accuracy of the focal plane determination by the CC method for particles in a real spray field. At first, a CCD camera was placed at position 1 (P1) and a hologram of a real droplet generated by an injector was obtained. Then, the CCD was moved to P2 and P3, consecutively taking holograms of the droplet at each position. The CCD was moved by a traverse system whose minimum resolution is 33 *nm*. Δd_1 and Δd_2 were then determined by the control software of the traverse system, which has enough precision for this study. The focal planes of these positions (d_{c1}, d_{c2}, and d_{c3}) are shown in Fig. 6 and were calculated using the CC method. The errors of these focal planes cannot be checked because the exact object distances are unknown, but Δd_1 can be compared to the difference between d_{c2} and d_{c1} because Δd_1 is known exactly from the traverse system measurement. If we assume d_{c1} is the exact object distance (d), d_{c2} can be compared with $d_{c1}+\Delta d_1$ and d_{c3} can be compared with $d_{c1}+\Delta d_1+\Delta d_2$. We can obtain the errors and validate the CC method for a real 3-D droplet using this procedure.

The hologram and reconstruction image of a droplet are shown in Fig. 7, and the errors of the focal plane determination for different sized droplets at different positions are shown in Fig. 8. The errors are generally proportional to the particle size, but all the errors exist within an acceptable range of tolerance, regardless of the droplet sizes. The results are also consistent with those discussed in the numerical simulation of holograms [11]. Thus, the CC method can be used as an appropriate tool for determination of the real 3-D droplets.

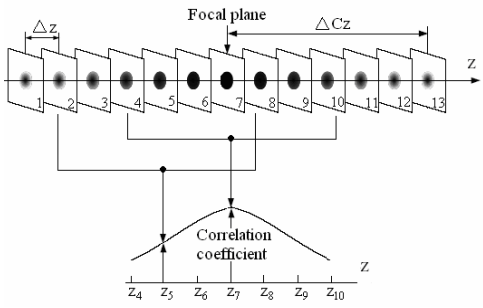

Fig. 5. Correlation coefficient method.

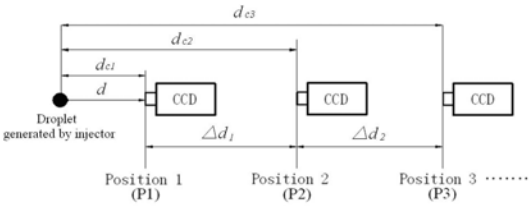

(a) Schematic of experiment

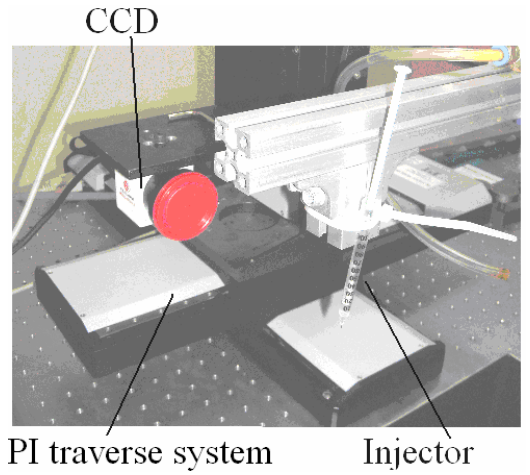

(b) Experimental equipment

Fig. 6. Validation experiments of the CC method for real 3-D droplets.

(a) (b) (c)

Fig. 7. Hologram and reconstruction image of a droplet; (a) hologram, (b) reconstruction image, (c) magnified image of (b).

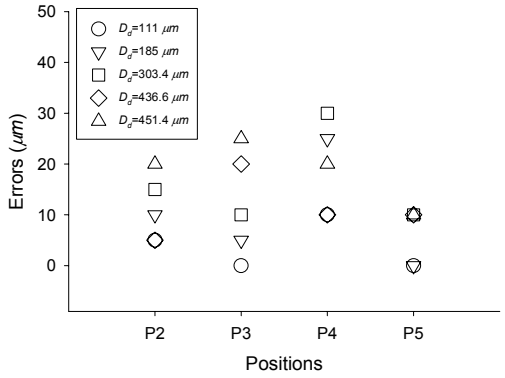

Fig. 8. Errors of the focal plane determination for different sized droplets at different positions.

3. Parameters of hologram recording

3.1 Object distance

In analyzing digital hologram recording procedures, the maximum spatial frequency method is frequently used [1]. The expression of maximum spatial frequency, $f_{\max}$, of in-line digital holography is

$$f_{\max} = \frac{1}{2\Delta x} = \frac{1}{2\Delta y} \tag{6}$$

where Δx and Δy are the pixel size or the resolution of holograms. The components of spatial frequency in the *x* and *y* directions are

$$f_x = \frac{x - \xi + d\sin\theta}{\lambda d}$$
$$f_y = \frac{y - \eta}{\lambda d} \tag{7}$$

where θ is the angle between the object beam and the reference beam [13]. The *x*, *y* coordinates of the boundaries of an object and a CCD plane are $\pm\xi_{\max}$, $\pm\eta_{\max}$, $\pm x_{\max}$, and $\pm y_{\max}$, respectively. Then, the maximum of f_x and f_y in Eq. (7) are

$$f_{x\max} = \frac{x_{\max} + \xi_{\max} + d\sin\theta}{\lambda d}$$
$$f_{y\max} = \frac{y_{\max} + \eta_{\max}}{\lambda d} \tag{8}$$

Combining Eqs. (6) and (8) with $\theta = 0$ for in-line digital holography, $\xi_{\max}$ and $\eta_{\max}$ are obtained as

$$\xi_{\max} = \frac{\lambda d}{\Delta x} - N\Delta x$$
$$\eta_{\max} = \frac{\lambda d}{\Delta y} - N\Delta y \tag{9}$$

where *N* is the pixel number.

In Eq. (9), we can find $\xi_{\max}$ and $\eta_{\max}$ are proportional to *d*. That is, the size of the object that can be recorded increases as the object distance increases. The size and number of pixels are usually fixed, namely, the size of the hologram (CCD size) is fixed. So, the resolution of the far-object hologram is smaller than that of the near-object hologram, although the recording size of a far-object is bigger than that of a near-object. This is similar to observing an object with our own eyes: we can see a whole and unclear object when a large object is far from us, but we can only see a partial object when the object is near to us, although it becomes clearer. Based on this, the object in digital particle holography should be as close to the CCD as possible.

The minimum object distance can be derived based on the distance condition of Fresnel diffraction [1],

$$d \geq \sqrt[3]{\frac{1}{4}\frac{[(\xi - x)^2 + (\eta - y)^2]^2_{\max}}{\lambda}} \tag{10}$$

Substituting $\Delta x = \Delta y = 7.4$ μm, $\lambda = 0.532$ μm, and $N = 2{,}048$ for the present study, the minimum object distance, $d = 173.25$ mm, is obtained. Thus, the object should be placed as close to the CCD camera as possible, but over this minimum distance.

3.2 Used region of laser beam

In this study, the expanded beam of a 10 cm diameter is much bigger than a CCD sensor (about 1.5 cm). So, only a small region of the expanded laser beam is used. Ideally, the expanded laser beam should have a Gaussian distribution, but the laser intensity cannot follow the ideal distribution in a real situation. The

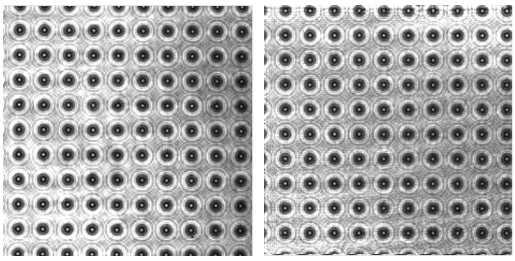

(a) (b)

Fig. 9. Holograms of a dot array target; (a) center region and (b) side region of beam.

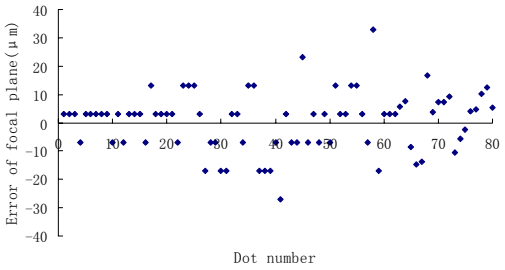

(a)

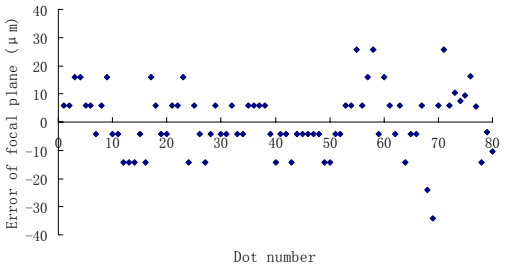

(b)

Fig. 10. Errors of focal plane determination; (a) center region and (b) side region of beam.

effect of using different regions of the laser beam on the CC method was examined. The holograms of a dot array target using the center region or the side region are shown in Fig. 9. Using these holograms and the CC method, the errors of focal plane determination are shown in Fig. 10. The mean values of errors using the center and side regions of the laser beam are 8.194 μm and 8.96 μm, respectively. The errors of both regions are acceptable and comparable to each other, but the use of the center region is preferable.

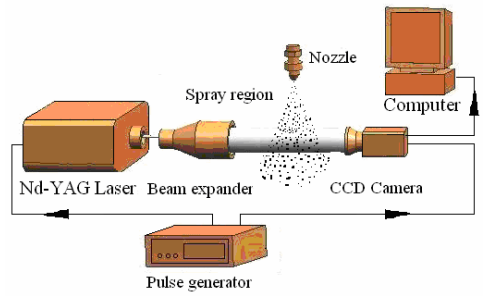

Fig. 11. Experiment setup for recording double exposure holograms of sprays.

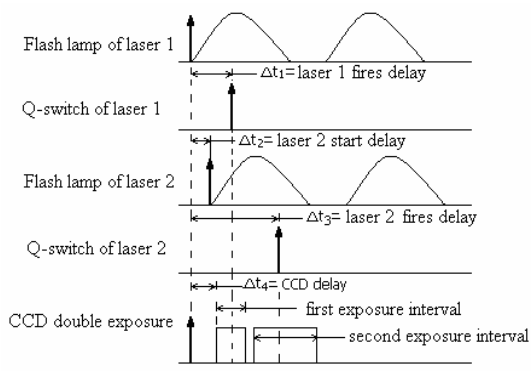

Fig. 12. Control diagram of synchronization system.

4. Spray experiments

4.1 Experimental setup and hologram recording

The experimental set-up for recording spray holograms is shown in Fig. 11. The control diagram of the synchronization system for the laser and the CCD camera is shown in Fig. 12. Each laser fires at Q-switches, with laser 2 delayed with respect to laser 1. If two lasers fire in the first and second exposure intervals of the CCD camera, two images can be obtained. The experimental conditions are as follows: the pixel size of the CCD camera is $\Delta\xi = \Delta\eta = 7.4$ μm; the pixel number N = 2,048; the distance between the nozzle and CCD camera d = 180 mm; the time interval of double pulse = 250 μs; and the spray injection pressure = 200 kPa. The double exposure spray holograms recorded are shown in Fig. 13.

4.2 Image reconstruction and post-processing

4.2.1 Thresholding

In digital particle holography, droplets are difficult to identify in the original reconstruction images of spray holograms because the grey values of droplets

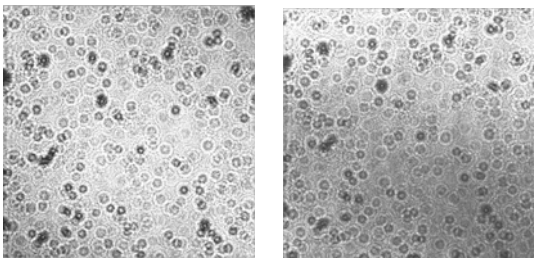

(a) (b)

Fig. 13. Spray holograms; (a) at first exposure, (b) at second exposure.

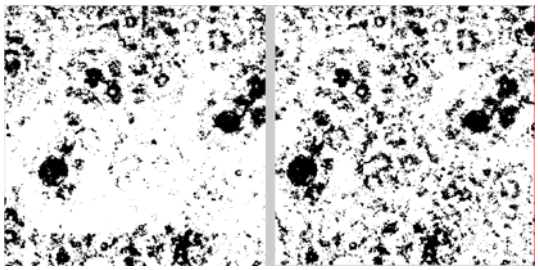

(a) (b)

Fig. 14. Comparison of binary images between (a) using different thresholds and (b) using one threshold.

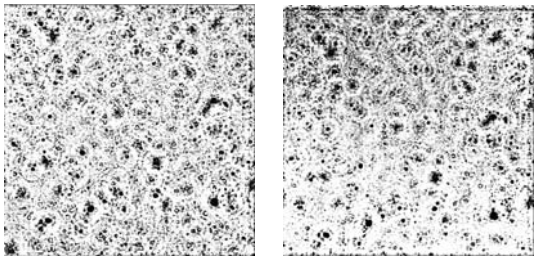

(a) (b)

Fig. 15. Binary images of reconstruction images; (a) at first exposure, (b) at second exposure.

are similar to those of the background. To obtain clear droplet images, appropriate threshold values should be determined to transform grey images to binary images. In this study, two threshold values are evaluated to obtain better results. The first threshold value, I_{th1}, is obtained as

$$I_{th1} = I_{1\min} + \bar{I}_1 \tag{11}$$

where $I_{1\min}$ and $\bar{I}_1$ are the minimum and average grey values of the reconstruction image, respectively. For the second threshold value, I_{th2}, the pixels whose grey values are under I_{th1} are selected first, comparing I_{th1} with the grey values of every pixel. The new minimum and average grey values of these pixels are $I_{2\min}$ and $\bar{I}_2$, respectively. The second threshold value is obtained as

$$I_{th2} = I_{2\min} + \bar{I}_2 \tag{12}$$

Using the second threshold value, we can transform grey images to binary images.

4.2.2 Image segmentation

Some useful information about particles can be lost if only one threshold is applied to the entire image because the intensity of the image is not uniform. Thus, image segmentation is used in this study. The entire image is divided into several small regions which are converted to binary images using different thresholds obtained by Eq. (12). Comparison of binary images using different thresholds and only one threshold is shown in Fig. 14; this clearly demonstrates that the image obtained by different thresholds is better than that by one threshold. Based on the two-threshold and the image segmentation methods, the final binary images of reconstruction images for double exposure spray holograms were obtained and are shown in Fig. 15.

4.2.3 Particle pairing

For 3-D velocity measurements of spray droplets, we must know the *x*, *y*, *z* coordinates of each droplet in the double exposure images. To find the *x*, *y* coordinates of each droplet in double exposure images, we reconstruct the hologram at an arbitrary distance and obtain the 2-D coordinates of the center of every droplet image using simple image processing techniques, regardless of whether or not the image is in focus. We checked the feasibility of the CC method for real droplets as described in Section 2, and obtained the optimal parameters used in the CC method [11]. Therefore, we can determine the focal plane of each droplet, namely, the *z* coordinate of each droplet in the double exposure images.

From the binary images obtained by the two-threshold and the image segmentation methods, the 3-D coordinates of every droplet in each image of two pulses are easily obtained. Then, the next step is to pair the same particles between pulses. We adopted Baek and Lee's method of neighboring match

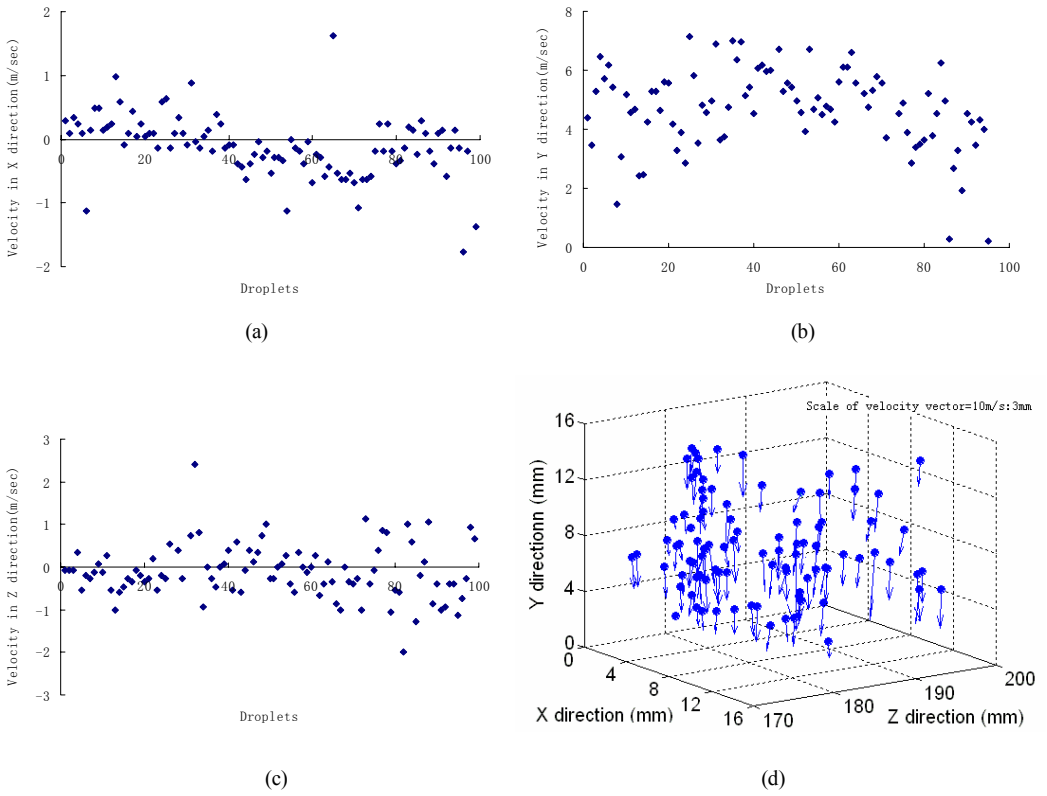

Fig. 16. Spatial velocities of spray droplets; velocities in (a) x direction, (b) y direction, (c) z direction, and (d) velocity vectors.

probability [14]. The method is based on the maximum velocity theory and quasi-rigidity conditions. A more detailed description of this algorithm can be found in [14].

4.3 Velocities and sizes of spray droplets

Combining the 3-D coordinates of paired particles and the time interval of double exposure, the spatial 3-D velocities of droplets are obtained, as shown in Fig. 16. Using the focal plane of particles found by the CC method, the focused images of droplets are reconstructed from holograms. Then, the edge of a droplet is located and the number of pixels inside the edge is counted. From these results, the areas and diameters of droplets are calculated. The relation between droplet velocities and diameters is shown in Fig. 17.

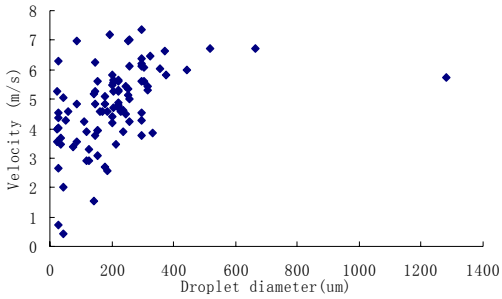

Fig. 17. Relation between velocities and sizes of droplets.

4.4 Uncertainty analysis

The particle velocity, V, are calculated by

$$V = \sqrt{V_x^2 + V_y^2 + V_z^2} \tag{13}$$

where V_x, V_y, V_z are the particle velocities in each direction, respectively.

The components of particle velocity in each direction are calculated by division of moved distances, D, by the time interval of double exposure, Δt. For x and y directions, the distance moved by a particle was obtained by multiplying the number of pixels between the center of particles at each exposure, ΔN, by the pixel size of CCD, Δ. They are expressed as

$$V_i = D_i / \Delta t = \Delta N_i \cdot \Delta i / \Delta t \qquad i = x, y \tag{14}$$

For z directions, the distance moved by a particle was the difference of the focal plane of the particle at each exposure. The velocity can be described as

$$V_z = (d_2 - d_1)/\Delta t \tag{15}$$

where d_1, d_2 are the focal planes of the particle along z direction in each exposure.

Based on the expression of uncertainties in measurement [15], the uncertainties of the particle velocity and each the velocity component are expressed as

$$u_V = \sqrt{\frac{V_x^2 u_{V_x}^2 + V_y^2 u_{V_y}^2 + V_z^2 u_{V_z}^2}{V_x^2 + V_y^2 + V_z^2}}$$
$$u_{V_i} = \sqrt{\left(\frac{\Delta N_i}{\Delta t} u_{\Delta i}\right)^2 + \left(\frac{\Delta N_i \Delta i}{\Delta t^2} u_{\Delta t}\right)^2 + \left(\frac{\Delta i}{\Delta t} u_{\Delta N_i}\right)^2} \tag{16}$$
$$i = x, y$$
$$u_{V_z} = \sqrt{\frac{u_{d_2}^2 + u_{d_1}^2}{\Delta t^2} + \frac{(d_2 - d_1)^2}{\Delta t^4} u_{\Delta t}^2}$$

In Eq. (16), the uncertainty of time interval of double exposure, $u_{\Delta t}$, approximates to zero because of the precision of the pulse generator and the laser machine. The uncertainty of the number of pixels, $u_{\Delta N_i}$, was assumed to be ±1 pixel. The uncertainty of pixel size, $u_{\Delta i}$, was assumed to be zero. The uncertainty of the focal plane position, u_{d1} and u_{d2}, can be obtained by the calibration target, after calculating the focal plane of particles in target 10 times. The uncertainty of the focal plane position was ±9.9 μm by using the method of type A evaluation of standard uncertainty [15].

Using the above uncertainties of related variables, the uncertainties of the velocities of all particles are calculated. The maximum uncertainty is ±0.296 m/s, which is 3.25% of the measured velocity, and the mean of all uncertainties is ±0.293 m/s.

The uncertainty of particle diameter measurement was also obtained using the calibration target. The particle area was calculated by multiplying the pixel number in image by the pixel size and then the diameter of particle was obtained from the area. Different size of particles was measured 10 times and the uncertainties of particle diameters are shown in Table 1. The maximum uncertainty is ±1.55 μm, which is ±0.4% of measured value. The maximum of error is 22.49 μm, which is 7.49% of actual diameter.

Table 1. Comparison of actual diameters and measured values.

Actual diameter (μm)	Measured diameter (μm)	Error (μm)
31	31.229 ± 0.98	1.229
70	71.045 ± 0.50	1.045
100	101.67 ± 0.84	1.67
160	161.71 ± 0.59	1.71
230	233.52 ± 1.02	3.52
300	322.49 ± 1.55	22.49

5. Conclusions

The potential of in-line digital particle holography as a method to measure the characteristics of spray droplets was presented. Based on preliminary experiments, the convolution method was chosen as the better reconstruction method. The influencing parameters at the time of hologram recording, such as the object distance and the region of laser beam used, were discussed. To obtain high quality holograms, we placed the object as close to the CCD camera as possible, but not closer than a certain minimum distance. Using the center region of laser beam produced better results. The feasibility of the correlation coefficient method for focal plane determination of 3-D droplets was verified.

The experimental setup to record spray holograms at two time moments was established with a synchronization system for time control, and two digital spray holograms within a short time interval were obtained. For post-processing of reconstruction images, the two-threshold and the image segmentation techniques were used in binary image transformation. After application of the correlation coefficient method and image processing techniques to droplets in each double exposure image, the spatial positions of the droplets used for the evaluation of droplet velocities could easily be located. The 3-D velocity and the size features of spray droplets were measured successfully using in-line digital particle holographic technology.

Acknowledgments

This work was supported by the Korea Research Foundation Grant funded by the Korean Government (KRF-2008-313-D00137).

References

[1] U. Schnars and W. Jueptner, *Digital Holography*, Springer, Berlin, Germany, (2005).

[2] M. Jaquot, P. Sandoz and G. Tribilon, High resolution digital holography, *Optics Communications*. 190 (1) (2001) 87-94.

[3] S. Lai, B. Kemper and G. V. Bally, Off-axis reconstruction of in-line holograms for twin-image elimination. *Optics Communications*. 169 (1) (1999) 37-43.

[4] H. Wang, D. Wang, J. Xie and S. Tao, Recording conditions of digital holography, *Proc. of International Congress on High-Speed Photography and Photonics*, SPIE, Bellingham, WA, USA. (2007) 62791J-1~10.

[5] J. Kim, J. Chu and S. Lee, Improvement of pattern recognition algorithm for drop size measurement, *Atomization and Sprays*. 9 (3) (1999) 313-329.

[6] K. J. Hay, Z. C. Liu and T. J. Hanratty, A backlighted imaging technique for particle size measurement in two-phase flows, *Experiments in Fluids*. 25 (3) (1998) 226-232.

[7] L. Yu and L. Cai, Iterative algorithm with a constraint condition for numerical reconstruction of three-dimensional object from its hologram, *J. Opt. Soc. Am. A*. 18 (5) (2001) 1033-1045.

[8] F. Dubois, C. Schockaert, N. Callens and C. Yourassowsky, Focus plane detection criteria in digital holography microscopy by amplitude analysis, *Opt. Express*. 14 (13) (2006) 5895-5980.

[9] C. B. Lefebvre, S. Coetmellec, D. Lebrun and C. Ozkul, Application of wavelet transform to hologram analysis: three-dimensional location of particles, *Opt. Laser Eng*. 33 (6) (2000) 409-421.

[10] Y. Zhang, D. X. Zheng, J. L. Shen and C. L. Zhang, 3D locations of the object directly from in-line holograms using the Gabor transform, *Proc. of Holography, Diffractive Optics, and Applications II*, SPIE, Bellingham, WA, USA. (5636) (2005) 116-120.

[11] Y. Yang, B. S. Kang and Y. J. Choo, Application of the correlation coefficient method for determination of the focal plane to digital particle holography, *Applied Optics*. 47 (6) (2008) 817-824.

[12] Y. J. Choo and B. S. Kang, The characteristics of the particle position along an optical axis in particle holography, *Meas. Sci. Technol*. 17 (4) (2006) 761-770.

[13] A. Macovsk, Spatial and temporal analysis of scanned systems, *Applied Optics*. 9 (8) (1970) 1906-1910.

[14] S. J. Baek and S. J. Lee, A new two-frame particle tracking algorithm using match probability, *Experiments in Fluids*. 22 (1) (1996) 23-30.

[15] *The Expression of Uncertainty and Confidence in Measurement*, United Kingdom Accreditation Service, M 3003, Edition 2, (2007) 16-36.

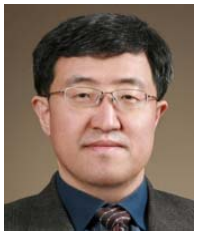

Boseon Kang received his B.S. and M.S. degrees in Mechanical Engineering from Seoul National University in 1986 and 1988, respectively. He then went on to receive his Ph.D. degree from University of Illinois, Chicago in 1995. He is currently Professor at School of Mechanical Systems Engineering, Chonnam National University in Gwangju, Korea. His research interests are in the area of sprays, holographic techniques in thermofluid measurements.

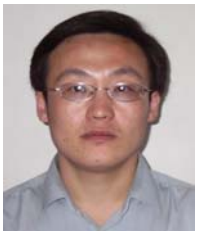

Yan Yang received his B.S. degree in Mechanical Engineering from Chongqing Insitute of Technology in 1997, and received his M.S. degree in Mechanics from Chongqing University in 2005. He is doctoral student of Department of Mechanical Systems Engineering, Chonnam National University in Gwangju, Korea. He is also currently Associate Professor at Automobile College, Chongqing University of Technology in Chongqing, China. His research direction is digital holographic techniques